Applied Microbiology and Biotechnology (2021) 105:5147–5158
https://doi.org/10.1007/s00253-021-11371-2

APPLIED MICROBIAL AND CELL PHYSIOLOGY

o-Vanillin, a promising antifungal agent, inhibits *Aspergillus flavus* by disrupting the integrity of cell walls and cell membranes

Qian Li[1] · Xiaoman Zhu[1] · Yanli Xie[1] · Yue Zhong[1]

Received: 2 December 2020 / Revised: 6 May 2021 / Accepted: 26 May 2021 / Published online: 4 June 2021

Abstract

o-Vanillin is a natural product that has been widely applied in the food and pharmaceutical industries. In this study, we determined that *o*-vanillin can strongly inhibit the growth of *Aspergillus flavus* mycelia. However, the inhibition mechanism of *o*-vanillin is still elusive. The ultrastructural morphology of mycelia was injured, and the cell walls were destroyed. The OH functional groups on cell walls were altered, and the content of protein in mycelial cell walls was reduced by *o*-vanillin. The content of β-1,3-glucan in cell walls was significantly ($P < 0.05$) reduced by *o*-vanillin in a dose-dependent manner, while chitin was not markedly affected. Moreover, *o*-vanillin led to an increase in the permeability of cell membranes. *o*-Vanillin also exhibited a promising antifungal effect on contaminated corn kernels. Therefore, *o*-vanillin inhibited the growth of mycelia by disrupting the integrity of cell walls and cell membranes. This study not only sheds light on the antifungal mechanism of *o*-vanillin but also indicates that it is a promising agent for the control of *A. flavus* infection.

Key points

- o-*Vanillin has strong inhibitory effects on A. flavus.*
- o-*Vanillin destroyed the integrity of cell walls and cell membranes.*
- o-*Vanillin could effectively inhibit the growth of A. flavus on corn kernels.*

Keywords *Aspergillus flavus* · *o*-Vanillin · Antifungal mechanism

Introduction

Aspergillus flavus is a common filamentous fungus that exists widely in plants and soils and can potentially contaminate grain crops, affecting approximately 25% of global crops (Klingelhöfer et al. 2018), e.g., peanut (*Arachis hypogaea* L.) and maize (*Zea mays* L.), and causing severe economic loss. In addition, *A. flavus* synthesizes and secretes aflatoxins as products of secondary metabolism, which are the most potent naturally induced hepatocarcinogens and therefore endanger the health of humans and livestock (Ali 2019). *A. flavus* is the second leading cause of aspergillosis in immunocompromised human patients with clinical symptoms such as nasosinusitis and keratitis (Hedayati et al. 2007; Chakrabarti and Singh 2011). Therefore, it is essential to develop methods to effectively and efficiently control the contamination of *A. flavus*.

At present, many investigations have been carried out to control the growth of *A. flavus*, including the application of physical, chemical, and biological methods. Atmospheric low-temperature plasma treatment (Dzimitrowicz et al. 2015) and antifungal peptides (Sadiq et al. 2019) exhibited good antifungal effects on *A. flavus* or aflatoxin degradation effects. Among chemical methods, synthesized preservatives (e.g., benzoic acid and its sodium salts, *p*-hydroxybenzoate esters) are neither environmentally friendly nor guaranteed to be safe for human health. In comparison with synthesized chemicals, natural products from plants and/or microbes have attracted great attention due to their numerous advantages, such as high yield, high effectiveness, low residual potential, and safety to the environment and human health (Falleh et al. 2020). Natural products, such as cinnamaldehyde and citral,

✉ Yanli Xie
ylxie@haut.edu.cn

[1] Henan Key Laboratory of Cereal and Oil Food Safety Inspection and Control, College of Food Science and Engineering, Henan University of Technology, Zhengzhou 450001, Henan, People's Republic of China

authorized by the Food and Drug Administration (FDA), have been applied as condiments in food and beverages (FDA 2021). Both cinnamaldehyde and citral have shown great antifungal effects against a broad range of fungi and restraining effects on the synthesis of aflatoxins (OuYang et al. 2019; Wang et al. 2019).

o-Vanillin (3-methoxysalicylaldehyde) is an active compound extracted from *Vanilla planifolia*, *Pinus koraiensis* fruit (Yi et al. 2015), and the *Helichrysum* genus (Esmaeili 2013). As an isomer of vanillin, *o*-vanillin has been extensively studied and applied in food, beverages, pharmaceuticals, and cosmetics (De et al. 2020). In addition, *o*-vanillin has a broad antimicrobial spectrum, including a variety of conditional pathogens, such as *Aspergillus* spp., *Cryptococcus neoformans*, and *Penicillium expansum* (Kim et al. 2011). The highest antifungal activity against *C. neoformans* was found for *o*-vanillin in comparison with vanillin and other vanillin derivatives (e.g., hydroxy/alkoxy benzaldehydes, halogenated benzaldehydes, and nitrated benzaldehydes) (Kim et al. 2014). Our recent study found that the antifungal efficacy of *o*-vanillin against spore germination of *A. flavus* is stronger than that of vanillin due to the relative positions of the functional groups (aldehyde, methoxy, and hydroxyl groups) (Li and Zhu 2021), which are similar to those facilitating mycelial growth. Therefore, *o*-vanillin is assumed to be a promising antifungal agent that can be applied for the postharvest preservation of grains, as well as in food processing. However, to the best of our knowledge, the inhibitory mechanism of *o*-vanillin against *A. flavus* is still unknown.

In this work, we first tested the susceptibility of *A. flavus* mycelia to *o*-vanillin. The influence of *o*-vanillin on cell walls and cell membranes was determined. The antifungal effect of *o*-vanillin on corn kernels was also evaluated. The novelty of this study is that we have determined that the components of cell walls and cell membranes serve as potential targets of *o*-vanillin in fighting *A. flavus*. All of these results are beneficial for us to understand the mechanism by which *o*-vanillin inhibits *A. flavus*, and the exploration of natural plant products will broaden the application spectrum of antifungal agents.

Materials and methods

Chemicals *o*-Vanillin (CAS: 148-53-8) was purchased from Aladdin Bio-Chem Technology Co. (Shanghai, China) and had a purity of 99% according to high-performance liquid chromatography. It was dissolved in 96.6% absolute ethanol and stored at 4°C in darkness. The final concentration of absolute ethanol in the culture medium was not higher than 2%. Vanillin (CAS: 121-33-5) was purchased from Aladdin Bio-Chem Technology Co. (Shanghai, China) with a purity of 99% by HPLC. Anti-fade mounting medium, glycine (CAS: 56-40-6), and methyl blue (CAS: 28983-56-4) were purchased from Sangon Biotech Co. (Shanghai, China). Calcofluor white (CAS: 4404-43-7) was purchased from Maokang Biotechnology Co. (Shanghai, China). Curdlan (CAS: 54724-00-4) was purchased from Macklin Biochemical Co. (Shanghai, China). Propidium iodide (PI) was purchased from Solarbio Science & Technology Co. (Beijing, China).

Fungal strain and the culture condition

The *A. flavus* strain (CGMCC 3.6304) was purchased from the China General Microbiological Culture Collection Center (CGMCC) and cultured with Sabouraud's dextrose agar (SDA), which contains 4% glucose, 1% peptone, and 2% agar, at 28 ± 2°C. One-week-old fungal cultures were ready to use in the following experiments.

Antifungal activity test

The susceptibility of *A. flavus* to *o*-vanillin was tested as described previously (Tao et al. 2014). *o*-Vanillin was mixed with SDA (10 mL) and poured into sterilized Petri dishes (60 mm diameter). The final concentrations of *o*-vanillin were 0, 25, 50, 75, and 100 μg/mL. Then, a 6-mm-diameter mycelial plug was inserted into an SDA plate, which was incubated at 28 ± 2°C for 72 h followed by colony measurement. The percentage of inhibition of mycelial growth (MGI) was calculated as follows:

$$\mathrm{MGI}\ (\%) = \frac{(\mathrm{dc}-0.6)-(\mathrm{dt}-0.6)}{\mathrm{dc}-0.6} \times 100$$

where d_c (cm) is the mean colony diameter for the control sets and d_t (cm) is the mean colony diameter for the treatment sets. The minimum inhibitory concentration (MIC) represented the minimum concentration at which the inhibition was 100% after 72 h. Vanillin was used as the positive control to evaluate the antifungal potential of *o*-vanillin. The method was the same as described above except for the final concentrations, which were 0, 160, 180, 200, 220, and 240 μg/mL.

Fresh spores were scraped from the solid culture plate and suspended in saline solution. The number of spores was counted with a hemocytometer and adjusted to 5×10^5 spores/mL. Spores (100 μL) were inoculated into 20 mL of Sabouraud's dextrose broth (4% glucose and 1% peptone, SDB) with shaking and cultured at 150 rpm and 28 ± 2°C for 24 h. Then, *o*-vanillin was added to reach final concentrations of 0, 25, 50, and 100 μg/mL, followed by another 24 h of culture (time point: 48 h). Mycelia were collected at 24 h as the 0-24 group and at 48 h as the 0-48, 25-48, 50-48, and 100-48 groups. The collected mycelia were dried at 80°C for 24 h and weighed. All experiments were performed at least three times in triplicate for each group.

Scanning electron microscopy (SEM)

A 100-μL spore suspension (5×10^5 spores/mL) was added to 20 mL of SDB and incubated at 28 ± 2°C for 24 h. Afterwards, *o*-vanillin was added to the culture medium to reach final concentrations of 0 (set as control), 50, and 100 μg/mL. After cultivation for another 24 h, samples were ready for SEM observation and the following assays. Mycelia were fixed in 2.5% glutaraldehyde for 12 h at 4°C. Afterwards, the samples were dehydrated in an ethanol series (30%, 50%, and 70%) for 15 min and then in 90% and 95% ethanol for 20 min. Then, the samples were dehydrated in an acetone series (25%, 50%, 75%, and 95%) for 10 min. Finally, isoamyl acetate and acetone were mixed in the indicated proportions (1:2, 1:1, 2:1, 1:0) and used as elution buffers (10-min elution for each buffer). The samples were dried with CO_2 critical point drying (K850, Quorum Technologies Ltd., Lewes, East Sussex, UK). After that, the dried samples were adhered to the sample stage with a conductive adhesive, and gold plating was sprayed using an ion sputtering sprayer (108auto, Cressington Scientific Instruments Ltd., Watford, UK). Samples were examined under a scanning electron microscope (Quanta 250 FEG, FEI, Hillsboro, OR, USA).

Transmission electron microscopy (TEM)

Mycelia were cultured and treated with *o*-vanillin as described above for SEM. Then, mycelia were fixed in 2.5% glutaraldehyde for 4 h at 4°C. Afterwards, mycelia were washed four times with phosphate buffer for 10 min followed by postfixation in 1.0% osmium tetraoxide for 2 h at 4°C. Samples were dehydrated in a graded ethanol series (50%, 70%, 80%, and 95%) and 100% acetone. They were soaked in a mixture of epoxy resin 812 and acetone (1:1, 1.5 h; 2:1, overnight) and then in epoxy resin 812 overnight. The specimens were embedded in Spurr's resin (SPI Supplies, West Chester, PA, USA). The polymerization process was as follows: 37°C for 12 h, 45°C for 12 h, and 60°C for 24 h. Ultrathin sections (approximately 70 nm) were prepared by an ultramicrotome with a diamond knife. The sections were mounted on copper grids and stained with saturated uranyl acetate and lead citrate (each 30 min). The samples were examined with a transmission electron microscope (JEM-14000, JEOL Ltd., Tokyo, Japan).

Fourier transform infrared spectroscopy (FT-IR)

Mycelia were first lyophilized into powder, and then the sample (1 mg) and 100 mg of KBr were placed into an agate mortar. After grinding and drying, the mixture was pressed into a sheet, and the surface functional groups were determined with an FT-IR spectrophotometer (Alpha, Bruker Corp., Karlsruhe, Germany) in the wavelength range of 400–4000 cm^{-1}. Pure KBr was used as the background, and the background absorption was subtracted by the difference spectrum technique.

X-ray photoelectron spectroscopy (XPS) assay

XPS spectra were collected using a K-Alpha XPS system (Thermo Fisher Scientific, East Grinstead, UK). The sample surfaces were etched for 30 s by argon gas before the XPS analysis to exclude the effect of impurities present on the surfaces of the samples. The base pressure in the analytical chamber was less than 5×10^{-7} Pa. The test parameters were set as follows: energy, 1486.8 eV; test spot area, 400 μm; tube voltage, 15 kV; tube current, 10 mA; and background vacuum, 2×10^{-9} mbar. The survey scans were collected for binding energy spanning from 1100 eV to 0 with an analyzer pass energy of 50 eV and a step of 1.00 eV.

Determination of β-1,3-glucan

The fluorescence dye-binding microassay for β-1,3-glucan was applied according to the method by Ko and Lin (2004) described previously. Lyophilized mycelial powder (5 mg) was suspended in 300 μL of NaOH (1 M) and 30 μL of NaOH (6 M), and then the mixture was incubated at 80°C for half an hour. Afterwards, samples were centrifuged at 4000*g* for 10 min, and then the supernatant was added to 630 μL of methyl blue mixture (40 v 0.1% methyl blue; 21 v 1 mol/L HCl; 59 v 1 mol/L glycine; pH 9.5) and incubated at 52°C for 30 min. The samples were further decolorized at room temperature for 30 min. The fluorescence intensity was measured with a fluorescence spectrophotometer (F-7100, Hitachi Ltd., Tokyo, Japan) at an excitation wavelength of 398 nm and an emission wavelength of 502 nm. The slit width was set as 10 nm for both excitation and emission. Curdlan was used as the standard for β-1,3-glucan calculation.

Determination of the chitin content

The content of chitin was determined as described previously (OuYang et al. 2019). Lyophilized mycelia (W_1) were added to saturated KOH and heated at 160°C for more than 15 min. When the samples became thin films, they were poured out and rinsed several times with distilled water. Afterwards, the samples were dehydrated with 95% ethanol and 96.6% absolute ethanol successively and weighed as W_2. The chitin content was calculated as:

Chitin content (%) $=W_2/W_1\times1.26\times100$where 1.26 represents the conversion factor of the relative molecular mass of *N*-acetamino-glucose/relative molecular mass of glucosamine.

Cell wall integrity test

A drop of fresh mycelium was added onto a glass slide, and the mycelia were stained with a drop of calcofluor white and 10% KOH. A drop of anti-fade mounting medium was also added onto the slide. Afterwards, samples were visualized under a fluorescence microscope (DFC 7000T, Leica Microsystems, Wetzlar, Germany).

Cell membrane integrity test

A drop of fresh mycelium was added onto a glass slide, and after twice washing with PBS, a drop of PI (1 μL/mL) was incubated with the mycelia for 20 min in darkness. After several times washing with PBS, the samples were visualized under a fluorescence microscope, and the fluorescence intensity was quantified by ImageJ software (1.52 v, National Institutes of Health (NIH), Bethesda, USA).

Release of cell constituents

The release of cell constituents was measured according to a method described previously (Zhou et al. 2014). Fifty microliters of spore suspension was inoculated into 10 mL SDB and shaking cultured for 24 h (150 rpm, 28 ± 2 °C). Then, mycelia were treated with *o*-vanillin at the concentrations of 0, 25, 50, and 100 μg/mL. After cultivation for another 24 h, the culture medium containing the released cell constituents was collected and centrifuged (8500 rpm/min, 10 min) to remove the free mycelia. The absorbance of the filtrate was measured at a wavelength of 260 nm with a UV/Vis spectrophotometer (UV-6100S, Mapada, Shanghai, China). SDB was used as the blank control.

Determination of relative conductivity and pH value

The determination of the relative conductivity was conducted as by the method described previously (Li et al. 2021). In brief, 5 mycelial plugs (diameter: 6 mm) from the margins of a 1-week-old plate were added to 100 mL SDB. After 24 h of shaking of the culture (150 rpm, 28 ± 2°C), the broth was treated with *o*-vanillin at concentrations of 0, 25, 50, and 100 μg/mL. After shaking the culture for another 24 h, mycelia were collected by gauze and washed several times with pure water (Wahaha, Hangzhou, China). After filtration in vacuum, 0.3 g of mycelia for each treated sample was suspended in 10 mL of pure water. The electrical conductivity of the sample in pure water was measured with a conductivity meter (DZS-706-C, INESA Scientific Instrument Co., Ltd, Shanghai, China) at 0, 5, 10, 20, 40, 60, 80, 100, 120, 140, 160, and 180 min. Afterwards, the mycelia were boiled for 10 min to measure the final conductivity. The conductivity of pure water was also measured before and after boiling as the background conductivity. The relative conductivity was calculated as:

$$\text{Relative conductivity}\ (\%) = \frac{\text{C1}-\text{Cw1}}{\text{C2}-\text{Cw2}} \times 100$$

where C_1 and C_2 represent the conductivities of *A. flavus* after the addition of *o*-vanillin before and after boiling, respectively. Cw_1 and Cw_2 represent the conductivities of pure water before and after boiling, respectively.

The pH value was measured immediately after conductivity at the above time points.

Antifungal test on corn kernels

Fresh corn kernels were washed with sterile water. After brief air drying, 3 corn kernels were placed into a Petri dish. Ten microliters of spore suspension (5×10^5 spores/mL) was injected into the corn kernels, and *o*-vanillin was added at final concentrations of 0, 25, 50, and 100 μg/mL. The corn kernels were incubated at 28 ± 2°C for 72 h, and the colony diameter of *A. flavus* was measured.

Statistical analysis

The results are presented as the mean ± SD. The significant differences between mean values were determined by one-way ANOVA using Duncan's multiple range test and Student's *t* test ($P < 0.05$). The statistical analyses were performed by using SPSS 20.0 (IBM, Armonk, USA).

Results

o-Vanillin inhibited the mycelial growth of *A. flavus*

The effect of *o*-vanillin on the mycelial growth of *A. flavus* is shown in Table 1. The morphologies of *A. flavus* colonies

Table 1 Antifungal activity of *o*-vanillin on *A. flavus*

Concentration (μg/mL)	Mycelial growth inhibition (%)		
	24 h	48 h	72 h
0	0.00±0.00 c	0.00±0.00 d	0.00±0.00 d
25	0.00±0.00 c	0.00±0.00 d	0.00±0.00 d
50	91.98±1.07 b	43.83±2.13 c	29.01±2.14 c
75	100.00±0.00 a	77.16±1.06 b	46.30±1.85 b
100	100.00±0.00 a	100.00±0.00 a	100.00±0.00 a
125	100.00±0.00 a	100.00±0.00 a	100.00±0.00 a

a–d significant difference ($P<0.05$) according to Duncan's multiple range test

within 72 h are shown in Supplementary Fig. S1. The mycelial growth of *A. flavus* was strongly inhibited by *o*-vanillin in a dose-dependent manner. After 72 h, the inhibition rates of *o*-vanillin at 50 μg/mL and 75 μg/mL were approximately 30% and 50%, respectively. At 100 μg/mL *o*-vanillin, the inhibition rate reached 100%. To further evaluate the effect of *o*-vanillin on mycelial growth in SDB, the mycelial weight after culture for 24 h and 48 h was measured. In Fig. 1A, mycelia grew strongly from 24 h to 48 h, as shown in the control group. Although mycelia could also grow significantly ($P < 0.05$) in the 25 and 50 μg/mL *o*-vanillin-treated groups, the increases were not as high as those in the control group. Complete growth inhibition was observed for the 100 μg/mL *o*-vanillin-treated group, the dry weight of which was close ($P > 0.05$) to that of the control at 24 h (0-24 group). Therefore, *o*-vanillin at 100 μg/mL exerted strong inhibition on *A. flavus* mycelia both on SDA and in SDB. As a comparison, the susceptibility of *A. flavus* in response to vanillin was also determined, and the MIC of vanillin was 240 μg/mL (Supplementary Fig. S2 and Supplementary Table S1), suggesting that the antifungal effect of *o*-vanillin was higher than that of vanillin. Direct optical visualization of mycelia is presented in Fig. 1B. Compared with the control, mycelia treated with *o*-vanillin displayed larger vacuoles (25 and 50 μg/mL groups) and even disordered cytoplasm (100 μg/mL group). Therefore, the dramatic inhibition of *o*-vanillin on mycelial growth of *A. flavus* was confirmed.

o-Vanillin changed the morphology of mycelia

To further characterize the ultrastructure of the mycelial surface, SEM was used to reveal the morphological alterations of mycelia. As shown in Fig. 2, the mycelia of the control group appeared strong and straight (Fig. 2A). However, *o*-vanillin at a concentration of 50 μg/mL induced irregular shrinkage of the mycelia (Fig. 2B). When the concentration increased to 100 μg/mL, the mycelia were obviously distorted and deformed, and a few of them were even broken (Fig. 2C). These results suggested that *o*-vanillin indeed changed the morphology of mycelia, and this effect was dose-dependent. Meanwhile, as seen in the insets of Fig. 2, mycelia in the control group were covered with an amorphous layer, also called fibrous decorations (Miyazawa et al. 2019), on the outer surfaces of the walls, while the surface of the *o*-vanillin-treated mycelia was smooth. In Fig. 3, TEM also revealed an amorphous layer on the surface of the control group (Fig. 3 A and C); however, this layer was severely injured on the mycelia treated with *o*-vanillin at 100 μg/mL (Fig. 3 B and D). Quantification analysis showed that the cell wall thickness of the control (n=5) was 151.22 ± 29.28 nm and that of the MIC group (n=5) was 109.88 ± 21.39 nm, which was significantly lower than that of the control group ($P < 0.05$).

OH groups were altered by *o*-vanillin (100 μg/mL)

To determine the structural differences of mycelial cell walls between the control and *o*-vanillin treatment groups, the functional groups of these samples were analyzed by FT-IR, as shown in Fig. 4A. The signal for the O–H stretching vibration in aromatic OH groups was observed at the broadly stretched absorption band at 3383 cm^{-1} (Fig. 4A-a). The signal for the symmetric stretching vibration of CH_3 occurs at 2923 cm^{-1} (Hua et al. 2020; Yang et al. 2020), as shown in Fig. 4A-b. Protein is one of the most important components of the cell wall. The two strong absorption peaks at 1655 cm^{-1} and 1556 cm^{-1} in the spectrum corresponded to the amide I band and amide II band, which are the characteristic infrared spectra of proteins (Fig. 4A-c and d) (Yuan et al. 2020). The absorption peak at 1076 cm^{-1} corresponded to C-C in the glucose chain (Fig. 4A-e). Compared with the peak at 3383 cm^{-1} for the 0, 25, and 50 μg/mL groups, the peak moved to a higher wavenumber of 3395 cm^{-1} for the group treated with *o*-vanillin at 100 μg/mL. Therefore, the OH groups in the 100 μg/mL *o*-vanillin-treated mycelia were altered.

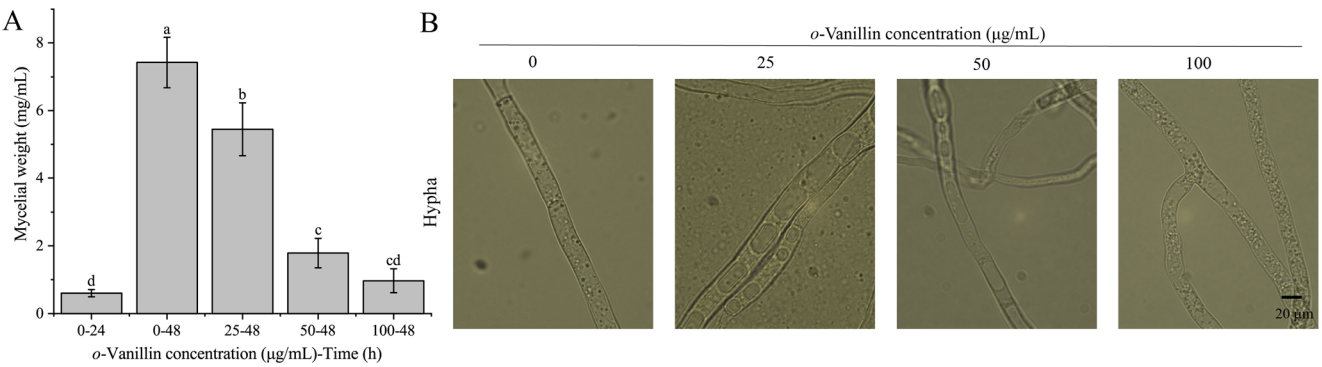

Fig. 1 Susceptibility of *A. flavus* in response to *o*-vanillin. **A** The mycelial dry weight. **B** The morphology of mycelial under an optical microscope. Scale bar: 20 μm

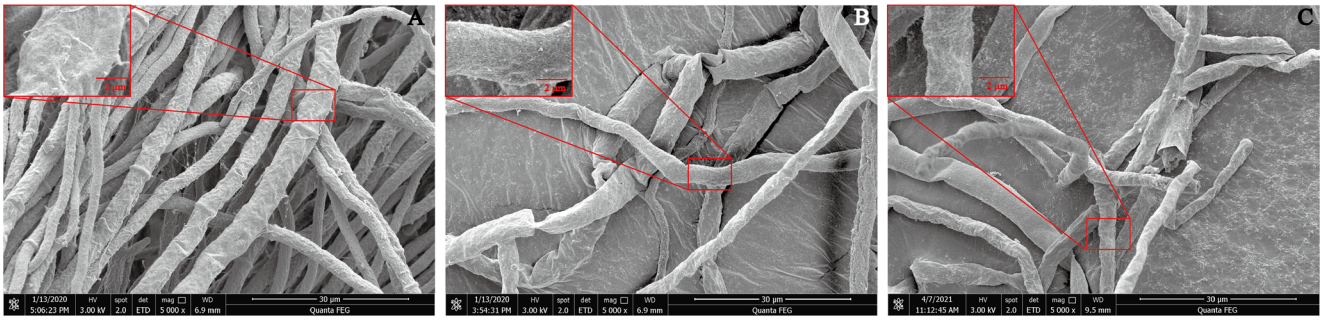

Fig. 2 SEM observation of mycelial morphology of *A. flavus* treated with *o*-vanillin at (**A**) 0, (**B**) 50 μg/mL, and (**C**) 100 μg/mL

o-Vanillin decreased the protein content of the cell wall surface

C, N, and O are three major elements in cell walls. To determine their changes, XPS was carried out. Figure 4B shows a typical XPS survey spectrum of *A. flavus* mycelia treated with or without *o*-vanillin (100 μg/mL). The C_{1s} peak for *A. flavus* surfaces can be decomposed into three components for carbon involved in C–(C, H) at 284.4 eV, C–(O, N) at 286.3 eV, and C=O bonds at 288.0 eV. The O_{1s} peak showed two components, with one attributed to O–C bonds at 532.7 eV and another attributed to O=C bonds at 531.4 eV. The N_{1s} peak consisted of two components: one component at 399.9 eV is attributed to amine or amide functionalities, and another component at 401.4 eV is attributed to protonated nitrogen (Supplementary Fig. S3). In comparison with the control group, the intensity of C and O did not change (Supplementary Fig. S3A&D, C&F), while the nitrogen intensity was significantly reduced from 9962.84 to 8011.29 in the 100 μg/mL *o*-vanillin group (Supplementary Fig. S3B&E). The relative distributions of C, N, and O atoms and the ratios of pairs of atoms were determined by analyzing the total area of the peaks and the corresponding photoemission cross sections. In Table 2, the contents of C, N, and O

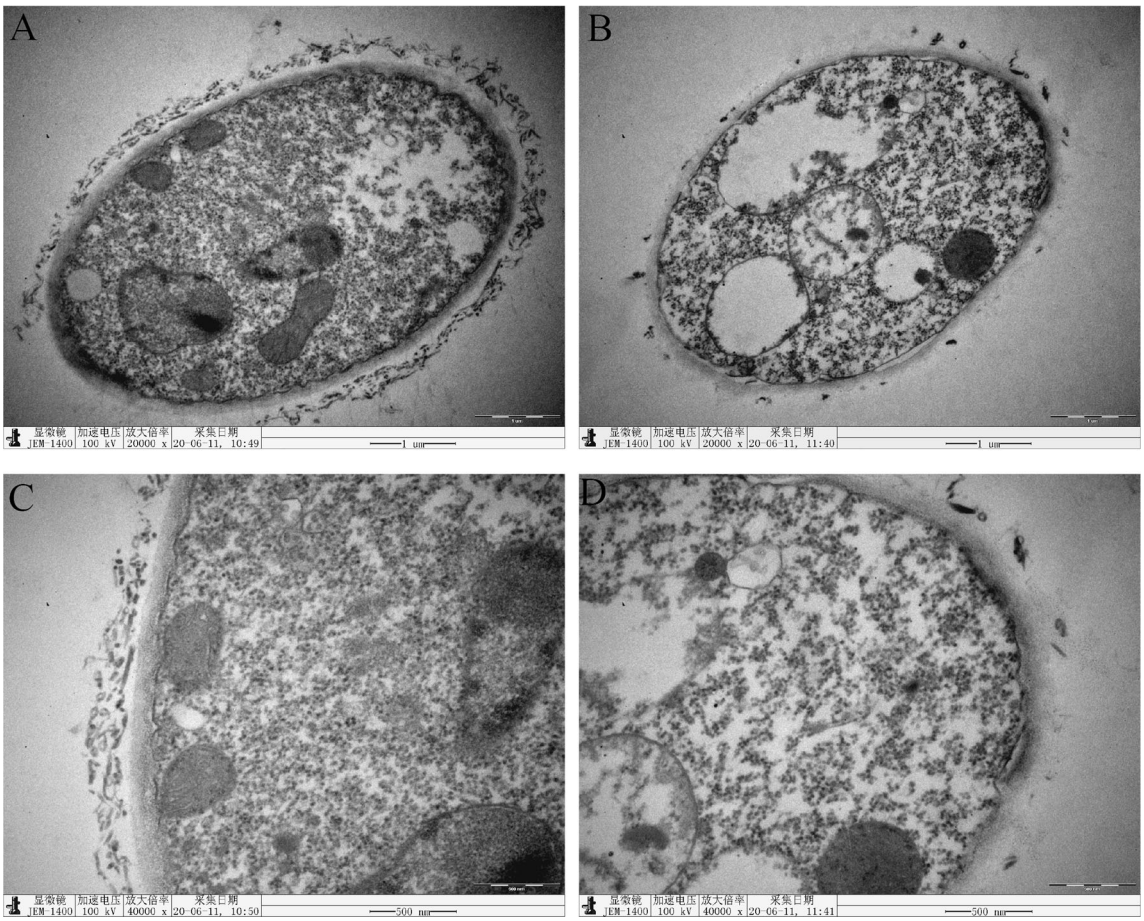

Fig. 3 TEM observation of mycelial morphology of *A. flavus* treated with *o*-vanillin at (**A**, **C**) 0 and (**B**, **D**) 100 μg/mL

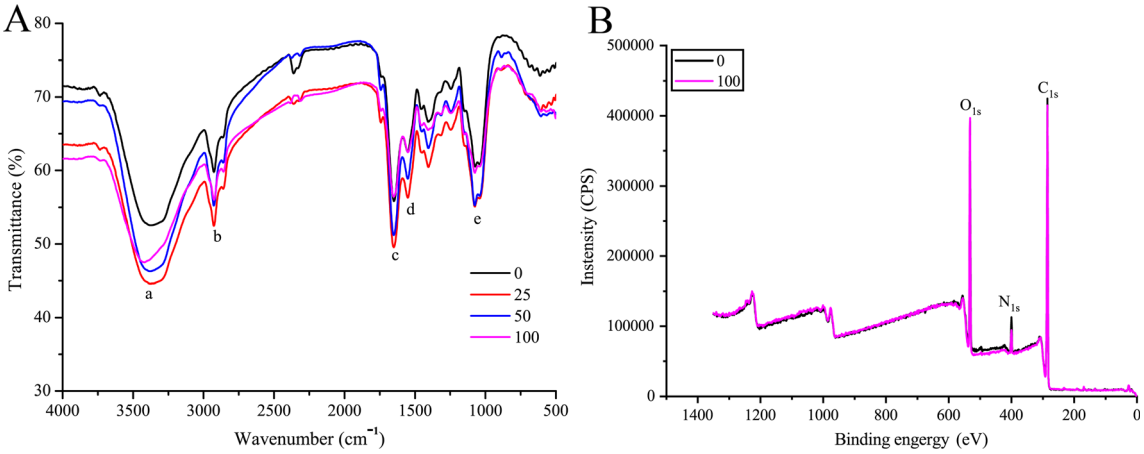

Fig. 4 Influence of *o*-vanillin on cell walls of *A. flavus*. (A) FT-IR spectra of mycelia treated with *o*-vanillin at 0, 25, 50, and 100 μg/mL. (B) XPS survey spectra of mycelia treated with *o*-vanillin at 0 and 100 μg/mL

fluctuated slightly after *o*-vanillin treatment; C% and O% increased, while N% decreased. C exists in proteins (Pr), polysaccharides (Ps), and lipids (Lp). To further decipher the change in C content due to *o*-vanillin treatment, the method reported by Dague et al. (2008) was used. The results showed that, in comparison with the control group, the ratio of C_{Pr} in the 100 μg/mL *o*-vanillin treatment group decreased by approximately 6%, while the increases in the ratios of C_{Ps} and C_{Lp} were not significant. Therefore, *o*-vanillin-treated mycelia contained fewer proteins.

The content of β-1,3-glucan but not chitin was decreased due to *o*-vanillin treatment

To quantify the effects of *o*-vanillin on the two main components of cell walls, β-1,3-glucan and chitin (Latgé et al. 2017), their contents were determined. The content of β-1,3-glucan decreased significantly due to *o*-vanillin treatment (Fig. 5A). The lowest concentration of *o*-vanillin (25 μg/mL) reduced the content of β-1,3-glucan by approximately 26%, and the higher the concentration of *o*-vanillin, the lower the content of β-1,3-glucan. The decreasing percentage of β-1,3-glucan for the 100 μg/mL group reached approximately 46%.

Chitin is another kind of polysaccharide of the cell wall component that maintains the cell wall integrity of fungi (Zhang et al. 2019). As shown in Fig. 5B, *o*-vanillin did not alter the content of chitin, which accounted for approximately 30% of the mycelia in all groups. Additionally, the distribution of chitin was determined by calcofluor white staining, which specifically labels chitin (Lewtak et al. 2014). Figure 5C-a shows that in the control group, chitin present in cell walls and septa (Rittenour et al. 2009) can be clearly visualized. In the other groups where mycelia were treated with *o*-vanillin, the septa seemed to be intact (Fig. 5C-b, c, and d). Quantification analysis (Supplementary Table S2) showed that although the number of septa was inhibited by *o*-vanillin in a dose-dependent manner, the inhibition percentages were not significant between the control group and all of the *o*-vanillin treatment groups ($P > 0.05$). Therefore, *o*-vanillin did not alter the chitin of *A. flavus*.

o-Vanillin destroyed cell membrane integrity

To test the effect of *o*-vanillin on the cell membrane of *A. flavus*, PI staining was conducted as described previously (Gao et al. 2016). Mycelia treated with *o*-vanillin showed intense red fluorescence, and with increasing concentrations of *o*-vanillin, the fluorescence intensity increased, indicating that *o*-vanillin gave rise to cell membrane destruction. In Table 3, *o*-vanillin at different concentrations of 25, 50, and 100 μg/mL increased the fluorescence values by approximately 1-, 6-, and 11-fold. The differences in fluorescence intensities between the *o*-vanillin treatment groups and the control

Table 2 Surface chemical composition measured by XPS of mycelia treated with *o*-vanillin at 0 and 100 μg/mL

Concentration (μg/mL)	%C	%N	%O	N/C	O/C	N/O	$\%C_{Pr}$	$\%C_{Ps}$	$\%C_{Lp}$
0	71.96	5.66	22.38	0.08	0.31	0.25	20.29	18.95	32.72
100	72.48	4.13	23.39	0.06	0.32	0.18	14.80	22.30	35.37

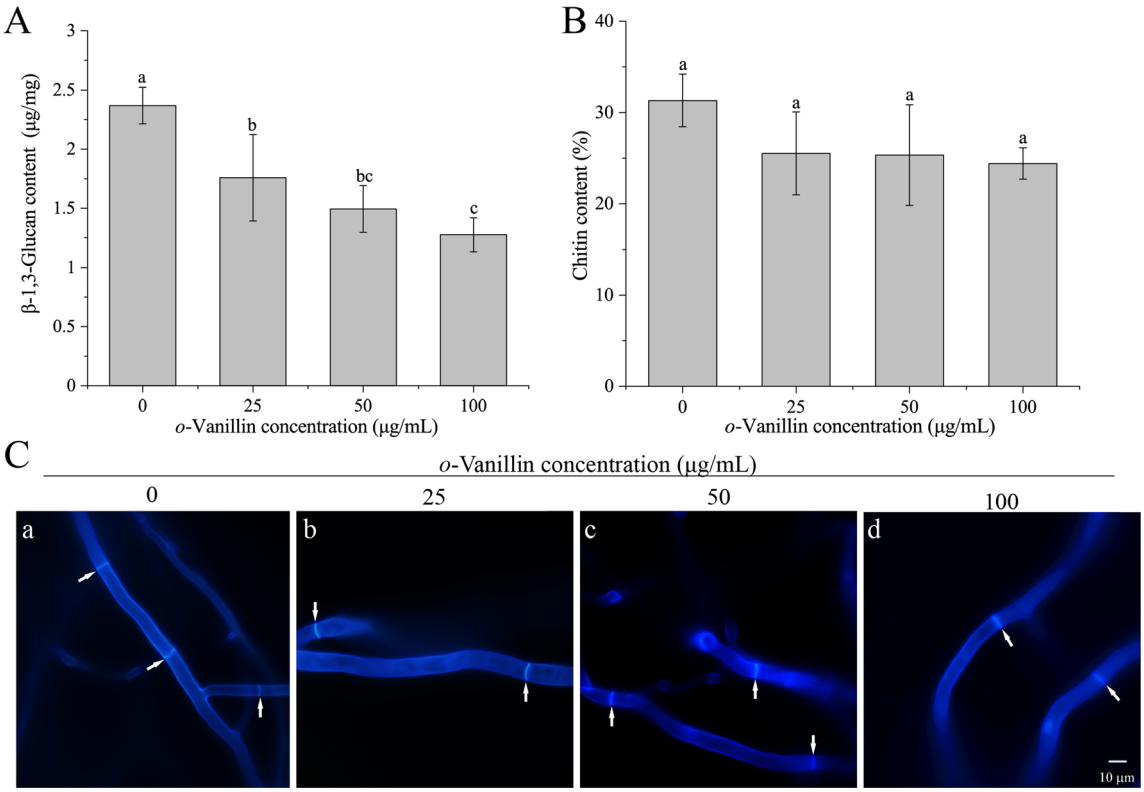

Fig. 5 Determination of the cell wall compositions of *A. flavus* treated with *o*-vanillin. (A) The content of β-1,3-glucan. (B) The content of chitin. (C) Mycelia treated with *o*-vanillin at 0, 25, 50, and 100 μg/mL after staining with calcofluor white under a fluorescence microscope. Scale bar: 10 μm

group were dramatic ($P < 0.05$), and the differences between the two treatment groups were also significant ($P < 0.05$).

Cell constituents were released after *o*-vanillin treatment

When the integrity of cell walls and membranes is compromised, there could be a leakage of celle constituents containing nucleic acids (Carson et al. 2002), the absorbance of which can be measured at a wavelength of 260 nm. In Table 3, *o*-vanillin induced the release of cell constituents significantly ($P < 0.05$), while the most obvious effect (about 50%) was observed for the 100 μg/mL *o*-vanillin treatment group. The result suggested that nucleic acids were released through a damaged cell wall and cell membrane.

Relative conductivity was increased and the extracellular pH value was decreased due to *o*-vanillin treatment

Figure 6 A shows that within 3 h after mycelia were vacuum dried, the relative conductivities increased over time for all groups regardless of whether they were treated with *o*-vanillin. With increasing concentrations of *o*-vanillin, the relative conductivity was obviously increased. The relative conductivities of mycelia for the control group and the 25 μg/mL *o*-vanillin treatment group were close throughout the test, indicating that the inhibition of *o*-vanillin at a low concentration was weak. The high relative conductivity (end time point: approximately 70%) of mycelia incubated with *o*-vanillin at 100 μg/mL was correlated with rapid electrolyte leakage, and this result suggested severe destruction of the cell barrier for this group.

Table 3 Effects of *o*-vanillin on the PI fluorescence intensity and the 260 nm absorbing material release of *A. flavus* at 0, 25, 50, and 100 μg/mL. The PI fluorescence of the control was set as 1

Concentration (μg/mL)	PI (fluorescence intensity/control)	Absorbance (OD_{260})
0	1.00±0.23 d	0.30±0.001 c
25	2.16±0.23 c	0.31±0.002 c
50	7.15±0.33 b	0.34±0.001 b
100	11.55±0.30 a	0.45±0.003 a

a–d significant difference ($P<0.05$) according to Duncan's multiple range test

To further determine the properties of ions released, the extracellular pH value was also tested. As shown in Fig. 6B, the overall pH value of the control group was always higher than those of the *o*-vanillin treatment groups. In general, the higher the *o*-vanillin concentration is, the lower the overall pH value. In addition, in comparison with the smooth curve of the pH value of the control group, the pH values of the treated groups showed an increasing trend during the test time. In addition, a downward trend within the first 5–10 min was observed for all groups. Therefore, the pH value results indicated that acidic acids comprised the majority of the extracellular environment.

Antifungal effect of *o*-vanillin in vitro on corn kernels

Table 4 shows that although the colony diameter of *A. flavus* was reduced by approximately 40% and 68% on corn kernels treated with *o*-vanillin at 25 and 50 μg/mL for 72 h, respectively, 100 μg/mL *o*-vanillin completely inhibited the growth of *A. flavus*. The growth of *A. flavus* on corn kernels is presented in Supplementary Fig. S4. Therefore, *o*-vanillin significantly prevented corn kernel contamination induced by *A. flavus*.

Discussion

Natural flavors extracted from edible plants have greatly intrigued researchers for many years due to their strong inhibitory effects on a variety of pathogens. Many natural flavors have been reported to inhibit spore germination and mycelial growth of *A. flavus*, such as cinnamaldehyde and citral (Sun et al. 2016; Moon et al. 2018). In addition to their antifungal effects, natural flavors have several positive properties, such as environmental friendliness, benefits for human health, and low cost (Pisoschi et al. 2018). Therefore, natural flavors have high potential to be applied in grains and foods as antifungal agents. *o*-Vanillin, as an isomer and a flavor substitute of vanillin, is added to food as a flavor and, most importantly, has been reported to fight against several kinds of fungi (Kim et al. 2011). However, the antifungal mechanism of *o*-vanillin against *A. flavus* is still ambiguous. In this study, we proposed that *o*-vanillin induced cell wall and cell membrane injury by reducing the content of β-1,3-glucan and cell permeability of *A. flavus* mycelia.

Table 4 *A. flavus* colony diameter on corn kernels treated with *o*-vanillin at 0, 25, 50, and 100 μg/mL

Concentration (μg/mL)	Colony diameter (cm)	Inhibition (%)
0	0.53±0.05 a	-
25	0.32±0.02 b	39.62
50	0.17±0.02 c	67.92
100	0.00±0.00 d	100.00

a–d significant difference ($P<0.05$) according to Duncan's multiple range test

The susceptibility test indicated that the proliferation of *A. flavus* was heavily restrained when the cells were exposed to *o*-vanillin. In this study, the MIC of *o*-vanillin on mycelial growth of *A. flavus* was 100 μg/mL, which was lower than that of vanillin (240 μg/mL). This value was close to those of the other vanillin isomers tested in our lab, such as HMB (2-hydroxy-4-methoxybenzaldehyde; 70 μg/mL) (Li et al. 2021) and 2-hydroxy-5-methoxybenzaldehyde (100 μg/mL) (Li and Zhu 2021), as well as extensively studied natural antifungal agents, such as thymol (80 μg/mL) (Shen et al. 2016) and cinnamaldehyde (104 μg/mL) (Sun et al. 2016), indicating that the antifungal effect of *o*-vanillin was extremely strong.

In the microimaging results, large vacuoles were observed in the mycelia treated with *o*-vanillin (Fig. 1B). This early formation of large vacuoles suggests the blockade of aflatoxin

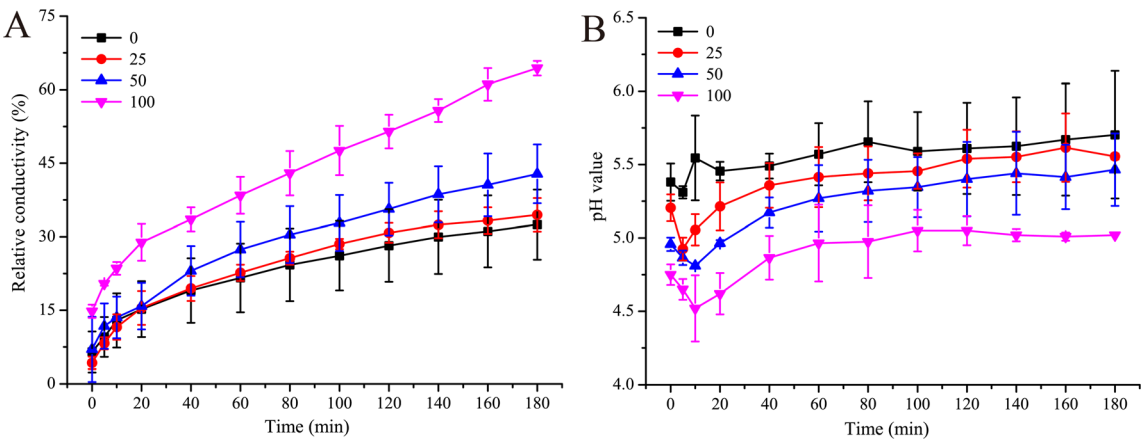

Fig. 6 Cell membrane permeability test of *A. flavus* treated with *o*-vanillin at 0, 25, 50, and 100 μg/mL. **A** Relative conductivity. **B** Extracellular pH value

synthesis and secretion, as reported by Chanda et al. (2010), in which the suppressed fusion of vesicles and vacuoles is considered the leading signal for the accumulation of aflatoxin. Similar large vacuole formation was also observed for glycoprotein-x (GPX)-treated *A. flavus* (Li et al. 2014). This phenomenon might also be associated with an elevated level of osmotic stress (Richards et al. 2010; Gao et al. 2016). Therefore, it is still necessary to determine whether the synthesis of aflatoxin is inhibited by *o*-vanillin and whether the formation of large vacuoles is directly associated with this inhibition.

The fungal cell wall is of great interest because it is absent from mammals and plays important roles in environmental resistance and host infection (Latgé 2010; Latgé et al. 2017). Therefore, the cell wall has been extensively studied and considered an antifungal target. Structural characterization reveals that it is schematically organized into two layers, of which the inner fibrous layer contains mainly glucans and chitin and is located adjacent to the plasma membrane, and the outer amorphous layer contains *N*-glycosylated proteins (Latgé 2010; Xie and Lipke 2010). One *N*-glycosylated protein identified in *Aspergillus* hyphae is galactosaminogalactan (GAG) (Garcia-Rubio et al. 2019), which, as a multifunctional virulence factor, mediates adherence to host cells (Gravelat et al. 2013). Deshmukh et al. (2020) reported that GAG can be secreted into the extracellular medium; therefore, we assume that GAG is also a component of the outer layers of *A. flavus.* Although a previous study claimed that cinnamaldehyde damaged the cell walls of *A. flavus* mycelia (Sun et al. 2016), this study, for the first time, reported that the plant-derived natural compound *o*-vanillin could strongly destroy both layers.

OH groups were altered due to *o*-vanillin treatment, where the O–H stretching vibration peak moved to a higher wavenumber (control: 3383 cm^{-1}, 100 μg/mL *o*-vanillin: 3395 cm^{-1}), indicating that some hydrogens in the hydroxyl groups were replaced, as explained previously by Serrano et al. (2010). Therefore, we hypothesized that *o*-vanillin altered the cell wall structure/components at 100 μg/mL. Further XPS results showed that the protein content in the mycelial surface was decreased by 27% by *o*-vanillin. In combination with the FT-IR results, *o*-vanillin influenced OH groups and destroyed proteins in the mycelial surface.

Apart from the outer layer, interestingly, *o*-vanillin destroyed the inner layer of *A. flavus* by reducing the content of β-1,3-glucan rather than chitin. These results are different from those previously reported for other plant-derived compounds. Belewa et al. (2017) found that extracts of *Tulbaghia violacea* reduced the content of both β-1,3-glucan and chitin and their respective synthases in *A. flavus*. OuYang et al. (2019) reported that cinnamaldehyde decreased the chitin content and expression levels of chitin synthase genes of *Geotrichum citri-aurantii*. In combination with the ultrastructural and physical characterization results, we assume that GAG and β-1,3-glucan are the potential antifungal targets of *o*-vanillin on *A. flavus*. However, whether the synthesis of GAG and β-1,3-glucan is suppressed or the degradation is promoted by *o*-vanillin requires further elucidation.

The cell membrane in fungi is an important cellular barrier that absorbs nutrition and exchanges material and energy with the surrounding environment. Its permeability and integrity play important roles in maintaining cell viability (Sant et al. 2016). Due to their hydrophobicity, many aldehydes bind to cell membranes with high affinity and induce the release of cell constituents (Burt 2004). Common parameters (PI fluorescence intensity, relative conductivity, and the content of cell constituents) were used to evaluate gross and irreversible damage to plasma membranes (Paul et al. 2011; Bajpai et al. 2013; Tao et al. 2014). In this study, the lowest concentration (25 μg/mL) initiated the loss of cell membrane integrity, which was reinforced for the 100 μg/mL treatment group. Similar damage to cell membranes was also found for citronellal-treated *Penicillium digitatum* (Wu et al. 2016) and citral-treated *Penicillium italicum* (*P. italicum*) (Tao et al. 2014). Meanwhile, the change in extracellular pH value indicated that *o*-vanillin treatment induced some alkaline ions to be released from mycelia, while in the control group, ions demonstrated a relatively balanced state. Our previous study showed a similar effect of HMB on the pH value of *A. flavus* (Li et al. 2021); citral, octanal, and α-terpineol decreased the pH value of *G. citri-aurantii* (Zhou et al. 2014), but citral and dill oil treatment increased the pH value of *P. italicum* (Tao et al. 2014) and *A. flavus* (Tian et al. 2012), respectively, and these values were much higher than that of the untreated mycelia, indicating that the intracellular antifungal targets were probably different for different compounds and/or pathogens. Kim et al. (2014) reported that *o*-vanillin inhibited *C. neoformans* by altering the function of transmembrane transport, providing direct evidence for the damage inflicted by *o*-vanillin on fungal cell membranes. Taken together, we confirmed that the cell membrane was irreversibly disrupted, ions inside the cells leaked, and the homeostasis of the osmotic pressure of the intra- and extracellular membranes was destroyed by *o*-vanillin treatment, especially when the applied concentration was above 50 μg/mL. Whether component(s) in the cell membrane are also antifungal target(s) of *o*-vanillin in *A. flavus* requires further elucidation. Moreover, the antifungal effects of *o*-vanillin on *A. flavus* appeared to be not proportional to their concentrations (the content of β-1,3-glucan, the fluorescence intensity of PI, etc.). Hence, illustrating the state of *o*-vanillin when it enters the cytoplasm of *A. flavus* is of interest. Finally, the promising inhibition of *o*-vanillin on the pathogenicity of *A. flavus* on corn kernels further proved that it is a potential antifungal agent in the preservation of grains.

In summary, the antifungal effect of *o*-vanillin on *A. flavus* could be attributed to the integrity disruption of cell walls (both the inner and outer layers) and cell membranes.

Identifying the precise antifungal target(s) is necessary to reveal the antifungal molecular mechanism of *o*-vanillin on *A. flavus* and to facilitate the application of *o*-vanillin in practice.

Supplementary Information The online version contains supplementary material available at https://doi.org/10.1007/s00253-021-11371-2.

Author contribution Q.L designed and coordinated the study. X.Z and Y.Z conducted experiments. X.Z wrote the initial draft of the manuscript. Y.X supervised the study. All authors read and approved the manuscript.

Funding This study was funded by the Innovative Funds Plan of Henan University of Technology (2020ZKCJ17), the Doctor Research Fund of Henan University of Technology (2019BS019), the Natural Science Research Projects of Education Department of Henan Province (21A550005), and Zhengzhou Key Science and Technology Innovation Project (2020CXZX0077).

Data availability The authors declare that (the/all other) data supporting the findings of this study are available within the article (and its supplementary information files)

Declarations

Competing interests The authors declare that they have no conflicts of interest.

Ethical statement This article does not contain any studies with human participants or animals performed by any of the authors.

References

Ali N (2019) Aflatoxins in rice: worldwide occurrence and public health perspectives. Toxicol Rep 6:1188–1197. https://doi.org/10.1016/j.toxrep.2019.11.007

Bajpai VK, Sharma A, Baek K-H (2013) Antibacterial mode of action of *Cudrania tricuspidata* fruit essential oil, affecting membrane permeability and surface characteristics of food-borne pathogens. Food Control 32(2):582–590. https://doi.org/10.1016/j.foodcont.2013.01.032

Belewa V, Baijnath H, Frost C, Somai BM (2017) *Tulbaghia violacea* Harv. plant extract affects cell wall synthesis in *Aspergillus flavus*. J Appl Microbiol 122(4):921–931. https://doi.org/10.1111/jam.13405

Burt S (2004) Essential oils: their antibacterial properties and potential applications in foods–a review. Int J Food Microbiol 94(3):223–253. https://doi.org/10.1016/j.ijfoodmicro.2004.03.022

Carson CF, Mee BJ, Riley TV (2002) Mechanism of action of *Melaleuca alternifolia* (tea tree) oil on *Staphylococcus aureus* determined by time-kill, lysis, leakage, and salt tolerance assays and electron microscopy. Antimicrob Agents Chemother 46(6):1914–1920. https://doi.org/10.1128/aac.46.6.1914-1920.2002

Chakrabarti A, Singh R (2011) The emerging epidemiology of mould infections in developing countries. Curr Opin Infect Dis 24(6):521–526. https://doi.org/10.1097/QCO.0b013e32834ab21e

Chanda A, Roze LV, Linz JE (2010) A possible role for exocytosis in aflatoxin export in *Aspergillus parasiticus*. Eukaryot Cell 9(11):1724–1727. https://doi.org/10.1128/EC.00118-10

Dague E, Delcorte A, Latgé JP, Dufrêne YF (2008) Combined use of atomic force microscopy, X-ray photoelectron spectroscopy, and secondary ion mass spectrometry for cell surface analysis. Langmuir 24:2956–2959. https://doi.org/10.1021/la703741y

De A, Ray HP, Jain P, Kaur H, Singh N (2020) Synthesis, characterization, molecular docking and DNA cleavage study of transition metal complexes of *o*-vanillin and glycine derived Schiff base ligand. J Mol Str 1199(5):126901. https://doi.org/10.1016/j.molstruc.2019.126901

Dzimitrowicz A, Jamróz P, Nowak P (2015) Sterilization by low-temperature atmospheric-pressure plasma. Postep Mikrobiol 54:195–200

Esmaeili A (2013) Biological activities and chemical composition of the stems and roots of *Helichrysum oligocephalum* DC grown in Iran. Pak J Pharm Sci 26(3):599–558. https://doi.org/10.1254/jphs.12250SC

Falleh H, Jemaa MB, Saada M, Ksouri R (2020) Essential oils: a promising eco-friendly food preservative. Food Chem 330:127268. https://doi.org/10.1016/j.foodchem.2020.127268

FDA (2021) Food and Drug Administration (FDA). Available online: https://www.accessdata.fda.gov/scripts/fdcc/index.cfm?set=FoodSubstances&id=HYDROXYMETHOXYBENZALDEHYDE. PUblisher. https://www.accessdata.fda.gov/scripts/fdcc/?set=FoodSubstances

Gao T, Zhou H, Zhou W, Hu L, Chen J, Shi Z (2016) The fungicidal activity of thymol against *Fusarium graminearum* via inducing lipid peroxidation and disrupting ergosterol biosynthesis. Molecules 21(6):1–13. https://doi.org/10.3390/molecules21060770

Garcia-Rubio R, Oliveira HC, Rivera J, Trevijano-Contador N (2019) The fungal cell wall: *Candida*, *Cryptococcus*, and *Aspergillus* species. Front Microbiol 10:2993. https://doi.org/10.3389/fmicb.2019.02993

Gravelat FN, Beauvais A, Liu H, Lee MJ, Snarr BD, Chen D, Xu WJ, Kravtsov I, Hoareau CMQ, Vanier G, Urb M, Campoli P, Abdallah AQ, Lehoux M, Chabot JC, Ouimet MC, Baptista SD, Fritz JH, Nierman WC, Latgé JP, Mitchell AP, Filler SG, Fontaine T, Sheppard DC (2013) *Aspergillus* galactosaminogalactan mediates adherence to host constituents and conceals hyphal beta-glucan from the immune system. PLos Pathog 9(8):e1003575. https://doi.org/10.1371/journal.ppat.1003575

Hedayati MT, Pasqualotto AC, Warn PA, Bowyer P, Denning DW (2007) *Aspergillus flavus*: human pathogen, allergen and mycotoxin producer. Microbiology 153(Pt 6):1677–1692. https://doi.org/10.1099/mic.0.2007/007641-0

Hua KC, Feng JT, Yang XG, Wang F, Zhang H, Yang L, Zhang HR, Xu MY, Li JK, Qiao RQ, Lun DX, Hu YC (2020) Assessment of the defatting efficacy of mechanical and chemical treatment for allograft cancellous bone and its effects on biomechanics properties of bone. Orthop Surg 12(2):617–630. https://doi.org/10.1111/os.12639

Kim JH, Chan KL, Mahoney N, Campbell B, C. (2011) Antifungal activity of redox-active benzaldehydes that target cellular antioxidation. Ann Clin Microb Anti 10(23):23. https://doi.org/10.1186/1476-0711-10-23

Kim JH, Lee HO, Cho YJ, Kim J, Chun J, Choi J, Lee Y, Jung WH (2014) A vanillin derivative causes mitochondrial dysfunction and triggers oxidative stress in *Cryptococcus neoformans*. PLoS One 9(2):e89122. https://doi.org/10.1371/journal.pone.0089122

Klingelhöfer D, Zhu Y, Braun M, Bendels MHK, Brüggmann D, Groneberg DA (2018) Aflatoxin-publication analysis of a global health threat. Food Control 89:280–290. https://doi.org/10.1016/j.foodcont.2018.02.017

Ko YT, Lin YL (2004) 1,3-β-Glucan quantification by a fluorescence microassay and analysis of its distribution in foods. J Agric Food Chem 52(11):3313–3318. https://doi.org/10.1021/jf0354085

Latgé JP (2010) Tasting the fungal cell wall. Cell Microbiol 12(7):863–872. https://doi.org/10.1111/j.1462-5822.2010.01474.x

Latgé JP, Beauvais A, Chamilos G (2017) The cell wall of the human fungal pathogen *Aspergillus fumigatus*: biosynthesis, organization, immune response, and virulence. Annu Rev Microbiol 71:99–116. https://doi.org/10.1146/annurev-micro-030117-020406

Lewtak K, Fiolka MJ, Szczuka E, Ptaszynska AA, Kotowicz N, Kolodziej P, Rzymowska J (2014) Analysis of antifungal and anticancer effects of the extract from *Pelargonium zonale*. Micron 66: 69–79. https://doi.org/10.1016/j.micron.2014.06.001

Li Q, Zhu XM (2021) Vanillin and its derivatives, potential promising antifungal agents, inhibit *Aspergillus flavus* spores via destroying the integrity of cell membrane rather than cell wall. Grain & Oil Science and Technology. https://doi.org/10.1016/j.gaost.2021.03.002

Li H, Wang M, Hu L, Mo H, Pan D (2014) Study on mushrooms vellulose ferivatives inhibiting aflatoxin production by *Aspergillus flavus*. Science and Technology of Food Industry 35:174–177 in chinese. https://doi.org/10.13386/j.issn1002-0306.2014.20.029

Li Q, Zhu XM, Xie YL, Ren SL (2021) 2-Hydroxy-4-methoxybenzaldehyde inhibits the growth of *Aspergillus flavus* via damaging cell wall, cell membrane, manipulating respiration thus creating a promising antifungal effect on corn kernels. Int J Food Sci Tech 56(1):178–184. https://doi.org/10.1111/ijfs.14617

Miyazawa K, Yoshimi A, Sano M, Tabata F, Sugahara A, Kasahara S, Koizumi A, Yano S, Nakajima T, Abe K (2019) Both galactosaminogalactan and α-1,3-glucan contribute to aggregation of *Aspergillus oryzae* hyphae in liquid culture. Front Microbiol 10: 2090. https://doi.org/10.3389/fmicb.2019.02090

Moon YS, Lee HS, Lee SE (2018) Inhibitory effects of three monoterpenes from ginger essential oil on growth and aflatoxin production of *Aspergillus flavus* and their gene regulation in aflatoxin biosynthesis. Appl Biol Chem 61(2):243–250. https://doi.org/10.1007/s13765-018-0352-x

OuYang QL, Duan XF, Li L, Tao NG (2019) Cinnamaldehyde exerts its antifungal activity by disrupting the cell wall integrity of *Geotrichum citri-aurantii*. Front Microbiol 10:000555. https://doi.org/10.3389/fmicb.2019.00055

Paul S, Dubey RC, Maheswari DK, Kang SC (2011) *Trachyspermum ammi* (L.) fruit essential oil influencing on membrane permeability and surface characteristics in inhibiting food-borne pathogens. Food Control 22(5):725–731. https://doi.org/10.1016/j.foodcont.2010.11.003

Pisoschi AM, Pop A, Georgescu C, Turcus V, Olah NK, Mathe E (2018) An overview of natural antimicrobials role in food. Eur J Med Chem 143:922–935. https://doi.org/10.1016/j.ejmech.2017.11.095

Richards A, Veses V, Gow NAR (2010) Vacuole dynamics in fungi. Fungal Biol Rev 24(3-4):93–105. https://doi.org/10.1016/j.fbr.2010.04.002

Rittenour WR, Si H, Harris SD (2009) Hyphal morphogenesis in *Aspergillus nidulans*. Fungal Biol Rev 23(1-2):20–29. https://doi.org/10.1016/j.fbr.2009.08.001

Sadiq FA, Yan B, Tian F, Zhao J, Zhang H, Chen W (2019) Lactic acid bacteria as antifungal and anti-mycotoxigenic agents: a comprehensive review. Compr Rev Food Sci Food 18(5):1403–1436. https://doi.org/10.1111/1541-4337.12481

Sant DG, Tupe SG, Ramana CV, Deshpande MV (2016) Fungal cell membrane-promising drug target for antifungal therapy. J Appl Microbiol 121(6):1498–1510. https://doi.org/10.1111/jam.13301

Serrano L, Egüés I, Alriols MG, Llano-Ponte R, Labidi J (2010) *Miscanthus sinensis* fractionation by different reagents. Chem Eng J 156(1):49–55. https://doi.org/10.1016/j.cej.2009.09.032

Shen QS, Zhou W, Li HB, Hu LB, Mo HZ (2016) ROS involves the fungicidal actions of thymol against spores of *Aspergillus flavus* via the induction of nitric oxide. PLoS One 11(5):e0155647. https://doi.org/10.1371/journal.pone.0155647

Sun Q, Shang B, Wang L, Lu ZS, Liu Y (2016) Cinnamaldehyde inhibits fungal growth and aflatoxin B1 biosynthesis by modulating the oxidative stress response of *Aspergillus flavus*. Appl Microbiol Biot 100(3):1355–1364. https://doi.org/10.1007/s00253-015-7159-z

Tao NG, OuYang QL, Jia L (2014) Citral inhibits mycelial growth of *Penicillium italicum* by a membrane damage mechanism. Food Control 41:116–121. https://doi.org/10.1016/j.foodcont.2014.01.010

Tian J, Ban XQ, Zeng H, He JS, Chen YX, Wang YW (2012) The mechanism of antifungal action of essential oil from dill (*Anethum graveolens* L.) on *Aspergillus flavus*. PLoS One 7(1):e30147. https://doi.org/10.1371/journal.pone.0030147

Wang LQ, Jiang N, Wang D, Wang M (2019) Effects of essential oil citral on the growth, mycotoxin biosynthesis and transcriptomic profile of *Alternaria alternata*. Toxins (Basel) 11(10):11100553. https://doi.org/10.3390/toxins11100553

Wu YL, OuYang QL, Tao NG (2016) Plasma membrane damage contributes to antifungal activity of citronellal against *Penicillium digitatum*. J Food Sci Technol 53(10):3853–3858. https://doi.org/10.1007/s13197-016-2358-x

Xie X, Lipke PN (2010) On the evolution of fungal and yeast cell walls. Yeast 27(8):479–488. https://doi.org/10.1002/yea.1787

Yang N, Qiu F, Zhu F, Qi L (2020) Therapeutic potential of zinc oxide-loaded syringic acid against in vitro and *in vivo* model of lung cancer. Int J Nanomedicine 15:8249–8260. https://doi.org/10.2147/IJN.S272997

Yi JJ, Wang ZY, Bai HN, Yu XJ, Jing J, Zuo LL (2015) Optimization of purification, identification and evaluation of the in vitro antitumor activity of polyphenols from *Pinus koraiensis* pinecones. Molecules 20(6):10450–10467. https://doi.org/10.3390/molecules200610450

Yuan K, Hu ZY, Chen KX, Lu C, Du LH (2020) Activity and mechanism of perilla essential oil in inhibiting *Aspergillus glaucus*. Food Science (in Chinese) 41(23):63–68. https://doi.org/10.7506/spkx1002-6630-20191103-022

Zhang J, Jiang H, Du Y, Keyhani NO, Xia Y, Jin K (2019) Members of chitin synthase family in *Metarhizium acridum* differentially affect fungal growth, stress tolerances, cell wall integrity and virulence. PLoS Pathog 15(8):e1007964. https://doi.org/10.1371/journal.ppat.1007964

Zhou HE, Tao NG, Jia L (2014) Antifungal activity of citral, octanal and α-terpineol against *Geotrichum citri-aurantii*. Food Control 37: 277–283. https://doi.org/10.1016/j.foodcont.2013.09.057